

Organic semiconductor UV Photocathodes for Photosensitive Gaseous detectors

B.A Laghari^{1*}, A.H Moghal¹, I.A Ismaili², J.V.Grazeulvacious³, Fredrick C.Krebs⁴, A.KhaliqueRajpar¹, IftekharAhmed¹, Imran Ali Halepoto¹

^{1*}Detector development Laboratory Institute of Physics University of Sindh Jamshoro Pakistan,

²Institute of information technology university of Sindh Jamshoro Pakistan,

³Department of Organic Technology Kaunas University of technology, Lithuania, ⁴The Danish Polymer Centre RisøNational Laboratory Denmark.

Abstract: We have investigated suitability of creating four new solid organic semiconductor photocathodes for use in photosensitive gaseous detectors. A thin layer of material was deposited by using vacuum evaporation technique through auto 306 coating system. Quantum efficiency QE was measured in photo-spectral sensitivity region between 190 - 250nm. The encouraging results are obtained.

Key words: Gaseous Photon detectors, Photosensitive Semiconductors, Photocathodes, Quantum Efficiency, Ageing of Photocathodes

I. Introduction

Photosensitive gaseous detectors have an essential role in large number of the present day and future experiments operating in high energy physics, astrophysics, plasma diagnostic and nuclear medical imaging. Photosensitive vapors were first time introduced by J.Séguinot, Ypsilantis [1] and independently by Bogomolov [2] in multiwire proportional chambers (MWPC) for detection of photons. Since then great deal of efforts have been devoted to find materials which can be handled at room conditions and exhibit high enough quantum efficiency (QE) to measure the fast component of barium fluoride (BaF₂) [3]. Historically, several organic and organometallic photosensitive compounds have been investigated to find suitable vapor, liquid and solid phase photocathodes compatible with fast gaseous detectors [4], the vapors with the lowest ionization potential used in gaseous photon detectors in some experiments so far are tri-methyl amine (TMA)[5], ethyl ferrocene(EF) [6], Tri-ethyl- amine(TEA), and tetrakisDimethylamine ethylene(TMAE) (see ref.[7] and references there in). TMAE has highest QE of all the known photoconverting vapours; when coupled to good quality quartz windows, photons can be detected up to 160-220nm. Its vapour pressure is low at room temperature. Therefore, low quantity of vapours can be accommodated in detector atmosphere. Two different techniques can be applied, often combining them to guarantee good photon absorption probability: Firstly, incoming photons are made to cross long gas gap which introduces parallax errors in locating the conversion point; secondly, the photon detectors are operated at higher temperatures that cannot be envisaged for practical reasons, and to avoid damaging the important components of the electronic read-out systems of the detectors. The main disadvantage of TMAE is that it is chemically very reactive to oxygen and materials used in detector construction [8]. An alternate approach could be to use solid photocathodes. They have low ionization threshold. Since, the use of solid photocathodes is favorable for good time resolution, since all the photoelectrons are emitted from same distance from the collecting anode plane, so there is no parallax [9]. The QE of the CsI surpasses that of all known solid UV-Photocathodes(see ref. [10] and references there in). It is comparable to TMAE vapours [11] in the short wave length but is smaller by a factor of 2 above 190nm. In spite of that solid photocathodes can operate in gaseous atmospheres successfully, the performance of MWPCs with CsI photocathodes is limited by ageing, resulting in severe decrease in QE [12, 13] because of the bombardment of the positive ions on CsI layer; created in the Townsend avalanche process, namely the ion back flow to the photocathode IBF. The presence of CsI layer causes electrical instabilities of the MWPCs accompanied by long recovery time (about 1 day) [14], which are because of both IBF and the feedback photons created in the avalanche region. In order to overcome these problems, Gas electron multiplier GEM [15], was introduced by Fabio Sauli. GEM-based gaseous photon detectors [16], are inherently fast, because the signal is essentially created by the electron motion and, when multilayer of GEM structures are used, no photon feedback is present, while ions created in multiplication process are trapped in the intermediate layers and do not reach the photocathode thus ageing of photocathode is prevented. The detailed study of IBF for GEM-based gaseous photon detectors [17, 18] show that rates as low as 10⁻³ can be obtained only by applying very low electric field at the photocathode surface. This causes reduction in photoelectron collection efficiency. A gain of about 10⁵, have been maintained for GEM-based gaseous detectors in laboratory but such a high gain cannot be conserved in the environment of an

experiment. This is based on the fact that the Hadron Blind detector (HBD) [19, 20, 21] GEM detectors are being operated at a total gain of 5000 and that GEM trackers employed in experiments operate at gains close to 10^4 . Thick GEMs (THGEM), introduced simultaneously by different groups [22, 23, 24, 25] are electron multipliers derived from the GEM architecture, changing the geometrical parameters and the production technology. The characteristics of THGEM-based gaseous detectors fulfill the necessities of photon detectors for imaging applications; the large gain, the robustness, the production mechanism and the mechanical features [26] are beneficial. They can offer position resolution up to mm level [27]. Because of the use of sophisticated technology, reduction in material budget of THGEM-based detectors is not noticeable. An important problem is the possibility to achieve good photoelectron collection efficiency on the entire reflective photoconverter surface of THGEM detector. Trajectory simulations of THGEM detectors signify that when the additional applied field between the CsI coated THGEM face and an electrode placed above it points towards the electrode above the THGEM, some of the photoelectrons are collected there do not enter the avalanche chain and are lost. For zero additional applied field, all the trajectories enter the THGEM holes, while when the additional applied field points towards the photocathode, the resulting field at the photocathode surface is decreased and less number of photoelectron is extracted or the field is too weak to direct them into the THGEM holes. The low dipole field results in smaller additional applied field that causes a decrease in the photoelectrons collection efficiency. The performance forecast of the simulations is established by measurements [28]. At the moment, in spite of the remarkable developments gaseous photon detectors are still not applicable in experiments [29]. Most necessities of these devices match to those of vacuum-based detectors; as a result, fabrication of the large area, low cost gaseous photon detectors with good quantum and photoelectron collection efficiencies suitable for room condition operation is still questionable.

In this article we will present for the first time a measurement of the QE of four new air stable organic semiconductor materials, known for their low ionization potential: Vp81, Js35, Tetracene and 2,5-Bis(5-tert-butyl-benzoxazol-2-yl)Thiophene (BBOT), which we propose to be used in photosensitive gaseous photon detectors.

II. General Properties Of Photoemissive Materials

Properties of Vp81 and Js35

The samples of organic glass forming semiconductors Vp81 formula ($C_{47}N_3H_{55}$) and JS35 formula ($C_{40}N_2S_2H_{30}O_2$) with low values of ionization potentials 5.0 eV and 5.1 eV respectively were obtained [30] specially for use as photocathodes in gaseous photon detectors. These materials are nontoxic, Unexplosive and solid at room temperature [30]. The chemical structures of the materials are given in fig. 1a and 1b respectively.

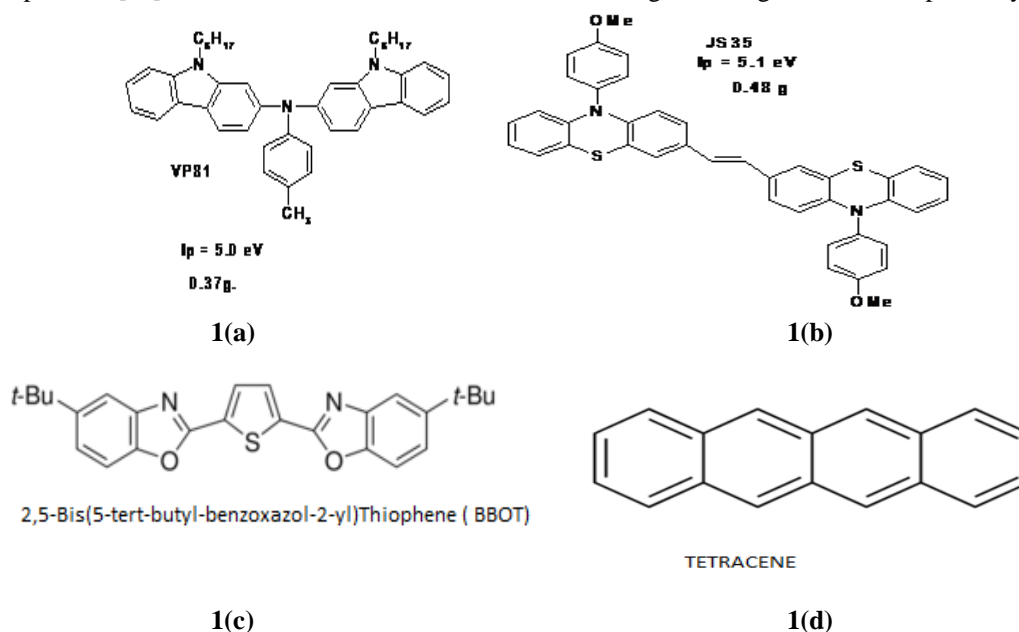


Figure:1 (a) The structure of organic semiconductors Vp81, (b) the structure of JS35, (c) the chemical structure of BBOT, (d) the chemical structure of Tetracene.

Properties Of Tetracene And BBOT

Tetracene and 2,5-Bis(5-tert-butyl-benzoxazol-2-yl) Thiophene (BBOT) is an air stable yellow to green powder, with ionization potential 5.9 eV, molecular formula $C_{26}H_{26}N_2O_2S$, molecular weight 430.56 gm/mole, melting point 199-201°C, non-toxic, Unexplosive and soluble in toluene. For chemical

structure see fig 1c. Tetracene is orange powder, with ionization potential 5.4 eV, molecular formula $C_{18}H_{12}$, molecular weight 228.29 gm/mol, melting point $>300^{\circ}C$, non-toxic, and Unexplosive. For chemical structure see fig. 1d. These materials were purchased from Sigma- Aldrich Co. LLC.

III. Experimental Set Up And Procedure

The basic experimental set up for QE measurement of photocathodes is shown in figure 2. It consists of prototype test detector made from stainless steel, developed for low current measurement, contained in the modified compartment of spectrophotometer (Shimadzu UV-1601), which limited the size of test detector to an external diameter of 7.5cm and an external length of 8.5cm, having a quartz window, area $21 \times 26 \text{mm}^2$ and thickness 2.16mm, a Hamamatsu photodiode (S1723-05) connected to a Keithley electrometer (model-6517A) for beam flux monitoring in situ, a second similar electrometer is used to collect photoelectrons produced by the photocathode and a turbo molecular pump system (BOC EDWARDS), which is used to pump the detector up to 2.3×10^{-4} Torr before the measurements. All the joints are sealed using Viton O-rings.

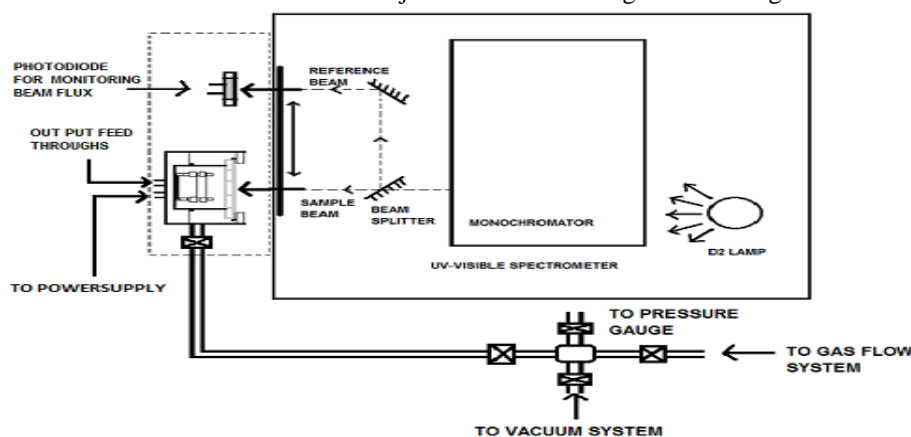


Figure 2 Schematic of basic experimental arrangement for QE measurement.

The schematic of prototype test detector is shown in figure 3. The electrical assembly of the test detector consists of a grounded circular copper plate, the photocathode under investigation is clipped on to it, two guard rings, in order to minimize edge effects and a guard ring-cum anode plane, spaced at 3mm by using fibre glass insulator spacers. The anode wire plane is made of $60\mu\text{m}$ diameter gold plated tungsten wires at pitch of 2mm to ensure a uniform electric field distribution in drift region.

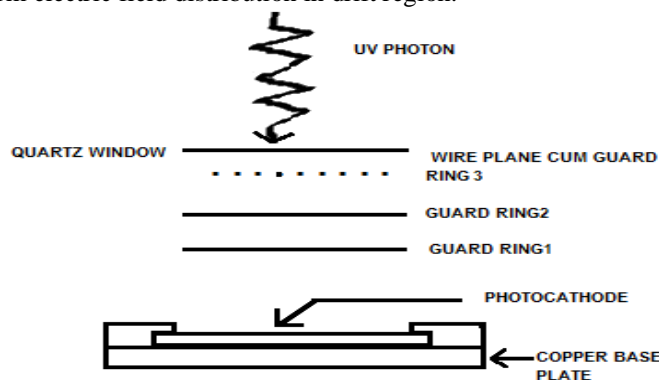


Figure 3 Schematic of prototype test detector.

Each wire is tensioned by a 50gms weight before soldered. The drift - gap is selected to be greater than four times the wire-pitch. The anode plane, guard rings and the metal plate are mounted PTFE studs using PTFE nuts and fibreglass insulator spacers to ensure electrically insulating properties and that the complete electrical assembly is free standing. The potentials of guard rings are defined using $1\text{M}\Omega$ thick film resistors. The electrical connection to the wire plane and photocathode are made using thick copper wires covered with PTFE sleeving, to avoid contact of signal carrying wires with chamber walls. The detector body is grounded through the screw connections on the base. Feedthroughs are positioned on the base of the detector. A guard ring design is used for the feed-throughs. LEMO connectors are soldered onto fibre-glass PCB. Four outer feeds- through pins secure the connector to the guard-ring on the reverseside of the board. A central pad inside the guard-ring

will feed the live signal through to the inside of the chamber. The solder provides primary vacuum seal. Epoxy resin is applied to a recess in which PCB is seated providing a secondary seal.

Before assembly, all the metallic components of prototype test detector were cleaned by sequential washing in acetone; detergent (Decon 90) and in ultrasonic bath in double distilled water.

This arrangement provides quick change-over of different photocathodes. A positive voltage (+25V) is applied in between anode plane and photocathode surface. .

IV. Calibration of Test facility

1. Photon flux calibration

The beam flux in both reference and sample beams of spectrophotometer (Shimadzu UV-1601), was determined by placing two UV-sensitive photodiodes (Hamamatsu S1723-05) in sample and reference beams respectively. These were reversed-biased at +5 volts to ensure linear response over the range of intensities. The photocurrents resulting from the incident light were measured with two electrometers (Keithley models-6517A). The photon flux at each photocathode was estimated by

$$N(\lambda) = \frac{P(\lambda)}{E(\lambda)S(\lambda)}$$

Where $N(\lambda)$ is the number of photons/s, $E(\lambda)$ is the energy of photon [J], $S(\lambda)$ is the diode sensitivity [A/W] and $P(\lambda)$ is the photocurrent [A] at wave length λ . For each photodiode, the photocurrent was determined from the relationship

$$P_x^y = S_x I_x$$

Where, P_x^y is the photocurrent of photodiode x in beam y , S_x is the sensitivity of photodiode x and I_x is the intensity of beam y . The quantity χ was then defined as

$$\begin{aligned} \chi &= \frac{I_{\text{sample}}}{I_{\text{reference}}} \\ &= \left[\frac{(I_{\text{sample}})^2}{(I_{\text{reference}})^2} \right]^{0.5} \\ &= \left[\frac{S_1 I_{\text{sample}}}{S_1 I_{\text{reference}} \frac{S_2 I_{\text{sample}}}{S_2 I_{\text{reference}}}} \right]^{0.5} \end{aligned}$$

Using photocurrent equation

$$\chi = \left[\frac{P_1^{\text{sample}}}{P_1^{\text{reference}}} \frac{P_2^{\text{sample}}}{P_2^{\text{reference}}} \right]^{0.5}$$

Thus, any variation in the measured intensity due to a discrepancy between the two photodiode's sensitivity or the difference between the beam flux in both the sample and reference beams was removed from the quantity χ . The variation in χ over the wave length region 190-280nm was found to be $\pm 1\%$.

2. Prototype test detector calibration

A. Measurement of optimum voltage

Measurement of optimum voltage was performed by using a copper photocathode, prepared from a piece of PCB, 2.3cm x 2.9cm cleaned with abrasion, rinsed with double distilled water (DD) then boiled in solution of Decon 90 in DD for 10 minutes, again washed with DD and dried. Photocathode prepared in this way was loaded in test chamber and detector was pumped to a vacuum of 2.3×10^{-4} Torr with turbo molecular pump BOC Edwards, irradiated with 200nm light from sample beam of UV spectrophotometer (Shimadzu UV-1601) and biasing voltage between anode plane and photocathode surface was varied from 0 to +40v, resulting photocurrent was recorded with Keithley electrometer (model-6517A). Fig.4 shows biasing voltage versus photocurrent graph. From plateau operating voltage was set to +25v.

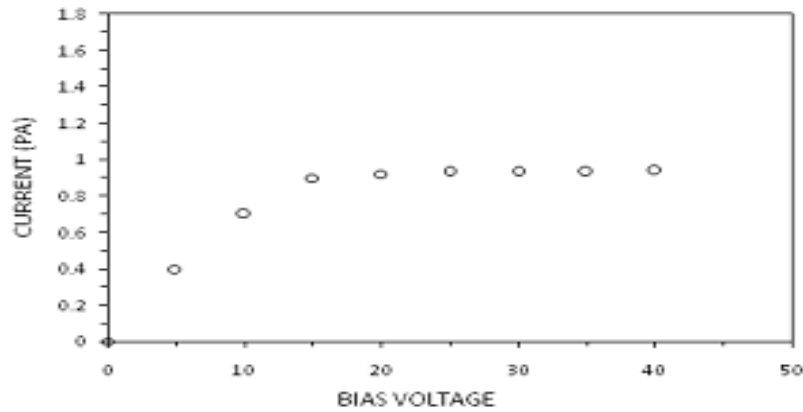


Figure 4 Pilot of biasing voltage versus photocurrent (measured in Pico amperes) when photocathode was irradiated with UV light wave length $\lambda=200\text{nm}$.

B. Calibration for QE measurement

Following equation was used for QE measurement of photocathodes:

$$QE = \frac{\text{No of photoelectrons}}{\text{No of photons}}$$

Where no of photoelectrons per second is given by

$$N_e = \frac{I_{dt}}{e}$$

Where I_{dt} detector is current in amperes and e is the charge of electron.

No of photons per second is given by

$$N_p = \frac{I_D}{D_s E_p}$$

Where I_D , D_s and E_p are photodiode current in amperes, photodiode sensitivity in amperes per watts and incident photon energy in joules respectively.

Prototype detector was calibrated for QE measurement by comparing QE curves of copper photocathode tested by CERN [31] with tested by our group, (fig 5a) and CsI tested by FERMI Lab [32] with tested by our group, (fig 5b).

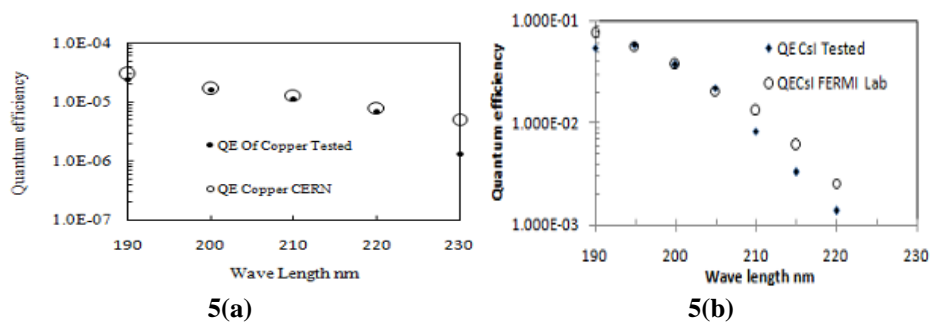


Figure 5 (a) comparison of QE of clean copper dots, with that of copper circles CERN [31] and (b) QE comparison curves of vacuum evaporated CsI photocathodes diamonds, with tested by FERMI Lab group circles [32].

Copper photocathode was prepared as described above and the CsI photocathode was prepared by vacuum evaporation technique using Auto 306 coating system (BOC Edwards). First a thin layer of about nm copper was deposited onto a borosilicate glass substrate 2.3cm×2.9cm. A 2.3cm×3mm of copper layer was masked with shutter for electrical contact and then about 500nm of CsI was deposited onto the remaining portion of the substrate at arate about 10-15nm/sec. Though the QE values of photocathodes tested by our group are less but the shape of the curves are similar which confirms proper operation of the prototype test detector.

V. Experimental Results and discussion

The quantum efficiency of the solid semiconductor Vp81 and JS35 photocathodes was measured in the range 190 to 250nm. The results are presented in fig. 6a: curve, dashed line with diamond is the sensitivity of clean copper cathode; curve, solid line with plus signs efficiency of the photocathode with a layer of about 500nm of Vp81 and in fig. 6b curve, dashed line with diamond is the sensitivity of clean copper and curve solid line with square efficiency of the photocathode with a layer of about 500nm of JS35, using vacuum evaporation technique.

The QE of solid vacuum evaporated photocathodes of Tetracene and BBOT, about 500nm thick are shown in fig. 6c and fig. 6d, measured in range 190-250nm.

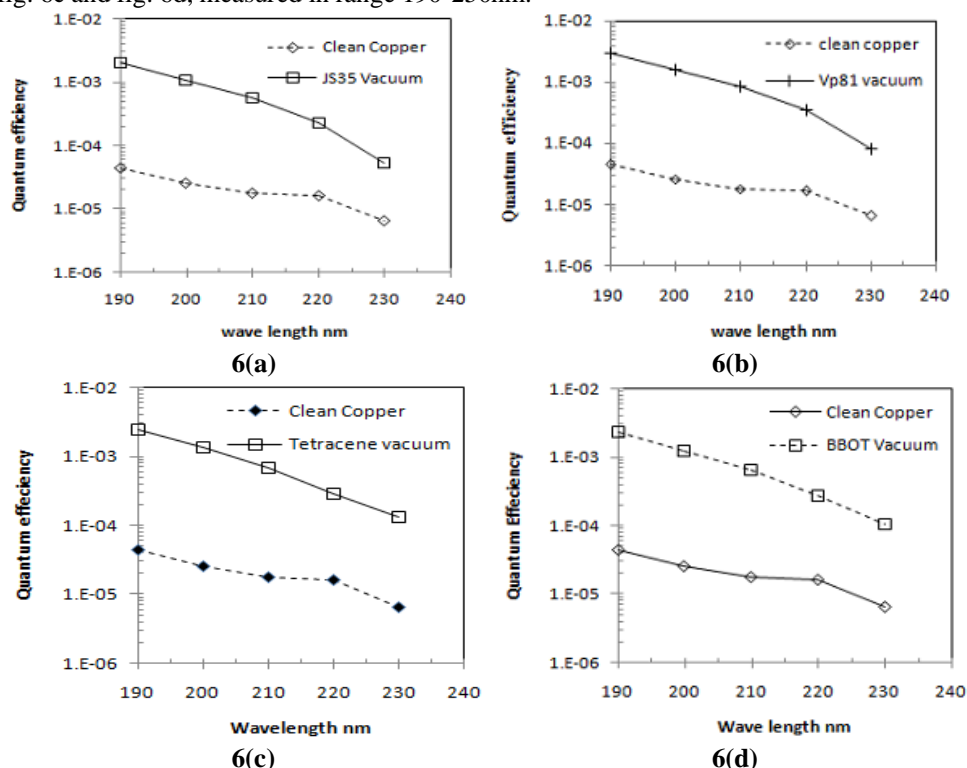
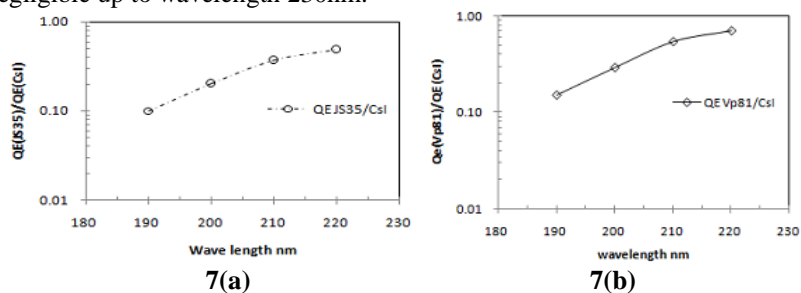


Figure 6 (a) Quantum efficiency of copper clean dashed line with diamond, Vp81 photocathode solid line with plus sign about 500nm thick, fabricated using vacuum evaporation technique, (b) QE of copper clean dashed line with diamonds, JS35 Photocathode solid line with squares, about 500nm thick, developed using vacuum evaporation technique, (c) QE of copper clean filled diamonds, Tetracene photocathode, approximately 500nm thick, squares and (d) QE of copper clean diamonds, BBOT photocathode squares, about 500nm thick, created using vacuum evaporation technique.

All of the above photocathodes remained stable during several days, a property that is favorable for practical applications. It can be seen that after deposition of the layers of Vp81, JS35, Tetracene and BBOT the efficiency of metallic cathodes increases, showing the layer effect. The absolute QE of these photocathodes in vacuum is non-negligible up to wavelength 230nm.



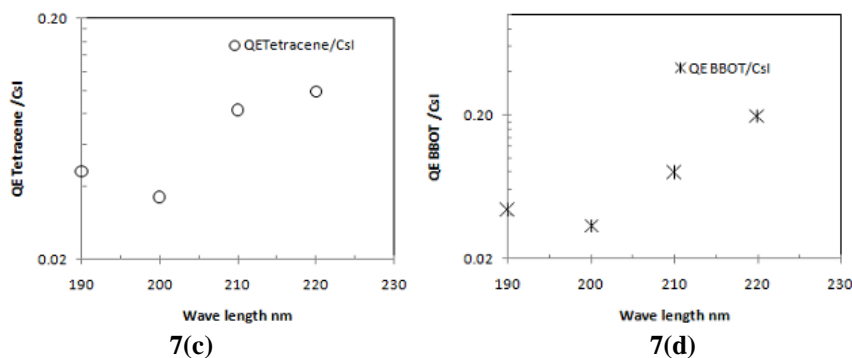


Figure 7 (a) QE of Vp81 photocathode relative to CsI for spectral range 190-220nm, (b) QE of JS35 photocathode relative to CsI for spectral range 190-220nm, (c) shows relative QE of Tetracene versus CsI for spectral range 190-220nm and (d) relative QE of BBOT as compared to CsI photocathode (as measured in our prototype detector) for spectral range 190-220nm .

A comparison of QE of Vp81, JS35, Tetracene and BBOT photocathodes with CsI, measured in this work by the same apparatus is shown in fig.7a, fig. 7b, fig.7c, and fig.7d respectively. From these figures it can be concluded that the four photocathodes have 6%, 4%, 4.6% and 4.3% of QE of the CsI photocathode at wave length 190nm.

VI. Conclusion

All the measurements described above show that these organic semiconductor materials have non-negligible absolute QE in vacuum, for spectral range 190-230nm. The quantum efficiencies of Vp81, JS35, Tetracene and BBOT relative to CsI photocathode (as measured using our prototype detector), for wave length $\lambda=190\text{nm}$ are 6%, 4%, 4.6% and 4.3% respectively. Moreover, photocathodes remained stable for several days and are solid at room temperature, can be attractive for large area gaseous photon detectors. Therefore these photocathodes can find application in some high energy experiments.

Acknowledgement

We would like to thank Prof. Dr. M. Yar Khuhawar for measurement of transmittance and absorption of quartz glass and his valuable suggestions about stability confirmation of these compounds. We would like to offer thanks to Dr. Taj Muhammad Jahangir Khuhawar for providing double distilled water and some solvents. Finally we would like to thank late Muhammad Naeem Memon for his technical assistance regarding construction of prototype detector and gas fittings.

References:

- [1]. J.Séguinot and T. Ypsilantis, Photoionization and Cherenkov Ring Imaging, Nucl. Instr. And Meth. 142 (1977) 377.
- [2]. G.D.Bogomolov, Yu.V.Pubrovskoe, and V.D.Peskov, Multiwire Gas counter for coordinate measures in the vuv region, Instr Exp.Tech,21(1978)778
- [3]. J Ph. Miné, G. Malamud, D. Vartsky, G. Vasileiadis, Organic UV photocathodes for gaseous particle detectors, Nucl.Instr. And Meth. A387 (1997) 171-175.
- [4]. G. Charpak, V. Peskov, F. Sauli, Preliminary results of the study of gaseous detectors with solid photocathodes sensitive in the spectral region from 105 to 300 nm, Nucl.Instr. And Meth. A323 (1992) 445-451.
- [5]. G.D.Bogomolov and V.D.Peskov, Multisectional Gas Counter for measurement of spectrum and polarization of x-rays, Prib.Techn.Exp.No 2(1981)212
- [6]. V.Peskov, Complex/Multiparameters plasma diagnostics in vuv and x-rays. Doctor of science thesis, (1982) keptza institution for physical problems USSR Academy of science, Moscow.
- [7]. J.Séguinot, The Cherenkov counters: Applications and limitations for identifying developments and prospects particles, CERN-EP 89-92-1989
- [8]. G. Charpak, V. Peskov, F. Sauli, D. Scigock Ethyl ferrocene in gas, condensed, or adsorbed phases: three types of photosensitive elements for use in gaseous detectors, Nucl.Instr. And Meth. A 277(1989)537
- [9]. G. Vasileiadis, G. Malamud, Ph. Miné, D. Vartsky, Solid and vapour phase UV photocathodes for gaseous detectors, Nucl.Instr. And Meth. A372(1996)31-34
- [10]. P. Miné, Photoemissive materials and their application to gaseous detector, Nucl.Instr. And Meth. A343(1994)99
- [11]. Richard A. Holroyd, Jack M. Preses, Craig L. Woody, Randy A. Johnson, Measurement of the absorption length and absolute quantum efficiency of TMAE and TEA from threshold to 120 nm, Nucl.Instr. And Meth.A261(1987)440
- [12]. Braem, G. De Cataldo, M. Davenport, A. Di Mauro, A. Franco, A. Gallas, H. Hoedlmoser, P. Martinengo, E. Nappi, F. Piu, E. Schyns, Results from the ageing studies of large CsI photocathodes exposed to ionizing radiation in a gaseous RICH detector, Nucl.Instr. And Meth.A.553(2005)187
- [13]. H. Hoedlmoser, A. Braem, G. De Cataldo, M. Davenport, A. Di Mauro, A. Franco, A. Gallas, P. Martinengo, E. Nappi, F. Piu, E. Schyn, Long term performance and ageing of CsI photocathodes for the ALICE/HMPID detector, Nucl.Instr.And Meth.A574(2007)28.

- [14]. E. Albrecht, G. Baum, R. Birsa, F. Bradamante, A. Bressan, A. Chapiro, A. Cicuttin, P. Ciliberti, A. Colavita, S. Costa, M. Crespo, P. Cristaudo, S. Dalla Torre, C. D'Ambrosio, V. Diaz, V. Duic, P. Fauland, M. Finger, F. Fratnik, M. Giorgi, B. Gobbo, et al, Status and characterization of COMPASS RICH-1, Nucl.Instr.And Meth. A.(553)215.
- [15]. F. Sauli, GEM: A new concept for electron amplification in gas detectors , Nucl.Instr. And Meth.A386(1997)531.
- [16]. D. Mörmann, A. Breskin, R. Chechik, C. Shalem, Operation principles and properties of the multi-GEM gaseous photomultiplier with reflective photocathode, Nucl.Instr. And Meth.A530(2004)258
- [17]. A Breskin, A Buzulutskov, R Chechik, B.K Singh, A Bondar, L Shekhtman, Sealed GEM photomultiplier with a CsI photocathode: ion feedback and ageing, Nucl.Instr.And Meth.A478(2002)225.
- [18]. A Bondar, A Buzulutskov, L Shekhtman, A Vasiljev, Study of ion feedback in multi-GEM structures, Nucl.Instr. And Meth.A496(2003)325.
- [19]. A. Kozlov, I. Ravinovich, L. Shekhtman, Z. Fraenkel, M. Inuzuka, I. Tserruya, Development of a triple GEM UV-photon detector operated in pure CF4 for the PHENIX experiment, Nucl.Instr.And Meth. A 523(2004)345.
- [20]. Z. Fraenkel, A. Kozlov, M. Naglis, I. Ravinovich, L. Shekhtman, I. Tserruya, B. Azmoun, C. Woody, S. Sawada, S. Yokkaichi, A. Milov, T. Gunji, H. Hamagaki, M. Inuzuka, T. Isobe, Y. Morino, S.X. Oda, K. Ozawa, S. Saito, T. Sakaguchi, Y. Yamaguchi, et al., A Hadron blind detector for the PHENIX experiment at RHIC. Nucl.Instr.And Meth.A546(2005)466.
- [21]. A.Milov,et al., Construction and Expected performance of Hadron Blind Detector for the PHENIX Experimental at RHIC, J.phy. G :Nucl.part.phys.34(2007)S701.
- [22]. P.Jeanneret,., Time projection and chambers and detection of neutrinos, Ph.D thesis Neuchatel university (2001).
- [23]. L Periale, V Peskov, P Carlson, T Francke, P Pavlopoulos, P Picchi, F Pietropaolo, Detection of the primary scintillation light from dense Ar, Kr and Xe with novel photosensitive gaseous detectors, Nucl.Instr.And Meth.A478(2002)377-383.
- [24]. P.S.Barbeau, J.Miyammoto, and I.Shipsy, Towards Coherent Neutrino Detection using Low- Background Micro pattern Gas Detectors. IEEE NS-50(2003)1285.
- [25]. R. Chechik, A. Breskin, C. Shalem, D. Mörmann, Thick GEM-like hole multipliers: properties and possible applications, Nucl.Instr.And Meth.A535(2004)303.
- [26]. S.Dalla Torre, et al, Micropattern gaseous photon detectors for Cherenkov imaging counters, in: IEEE-2008 Nuclear science symposium and medical imaging conference,Dresden,19-25/10/2008.
- [27]. M. Cortesi, R.Alon, R.Chechik, A.Breskin, D.Vartsky and V.Dangendorf, Investigation of a THGEM based imaging detector, J.Instr.2(2002)p09002.
- [28]. M. Alexeev, R. Birsa, F. Bradamante, A. Bressan, M. Chiosso, P. Ciliberti, G. Croci, M.L. Colantoni, S. Dalla Torre, S. Duarte Pinto, O. Denisov, V. Diaz, V. Duic, A. Ferrero, M. Finger, M. Finger Jr, H. Fischer, G. Giacomini, M. Giorgi, B. Gobbo, F.H. Heinsius, et al., Micropattern gaseous photon detectors for Cherenkov imaging counters, Nucl.Instr. And Meth.A623(2010)129-131
- [29]. S. Dalla Torre, Status and perspectives of gaseous photon detectors, Nucl.InstrAnd Meth. A639(2011)111-116.
- [30]. J.V.Grazeulvacious, Department of organic Technology Kaunas University Lithuania, collaboration
- [31]. V. Peskov, G. Charpak, F. Sauli, D. Scigock V. Diep, D. Janjic, Organometallic photocathodes for parallel-plate and wire chambers, Nucl.InstrAnd Meth. A 283(1989)786-791
- [32]. A. Borovick-Romanov V. Peskov*, Cs based photocathodes for gaseous detectors, Nucl.InstrAnd Meth. A 348(1998)269-274